Inorganic Chemistry

Article

pubs.acs.org/IC

Oxozinc Carboxylate Complexes: A New Synthetic Approach and the Carboxylate Ligand Effect on the Noncovalent-Interactions-Driven Self-Assembly

Wojciech Bury,[†] Iwona Justyniak,*[,‡] Daniel Prochowicz,[†] Anna Rola-Noworyta,[‡] and Janusz Lewiński*[,†,‡]

[†]Faculty of Chemistry, Warsaw University of Technology, Noakowskiego 3, 00-664 Warsaw, Poland

[‡]Institute of Physical Chemistry, Polish Academy of Sciences, Kasprzaka 44/52, 01-224 Warsaw, Poland

Supporting Information

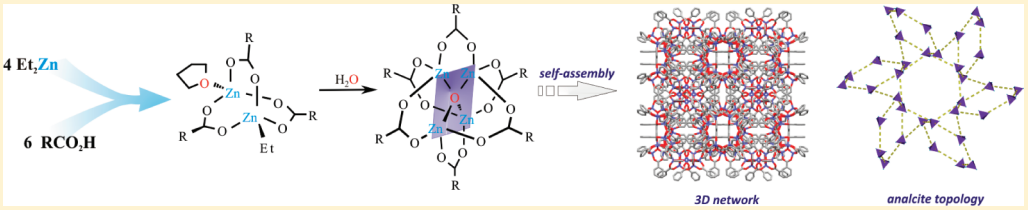

ABSTRACT: An atom-efficient and mild synthesis of a series of oxozinc carboxylates $[Zn_4(\mu_4\text{-}O)(O_2CR)_6]$ [where R = Ph (**2a**), *p*-PhC_6H_4 (**2b**), *p*-MeC_6H_4 (**2c**), and *p*-$MeSC_6H_4$ (**2d**)] from well-defined alkylzinc precursors and H_2O is described. The molecular and crystal structures of the resulting complexes have been determined by single-crystal X-ray diffraction. A closer examination of their crystal structure provides a direct picture of the effect of the nature of substituents on the molecular self-assembly of the octahedral oxozinc through noncovalent interactions. It was revealed that these discrete oxozinc clusters can form diverse types of noncovalent assemblies ranging from structures representing zeolitic topologies in the case of **2a** to soft porous materials with gated voids or open channels for the remaining molecular clusters.

INTRODUCTION

Zinc oxocarboxylates have been widely utilized as basic building units in a large class of microporous zinc-based metal−organic frameworks (MOFs).[1] Typically isoreticular MOF-type structures can be synthesized via solvothermal reaction of inorganic zinc salts with dicarboxylic acids. Recently oxozinc cluster was also applied as a very efficient predefined precursor for the synthesis of MOF-5 under mild conditions.[2] The $[Zn_4O]^{6+}$ nodal regions within these materials, which are of particular interest as promising hydrogen storage materials,[3] have been identified as the principal sites for the adsorption of a hydrogen molecule.[4] In addition, the potential capability of molecular oxozinc clusters for hydrogen adsorption was previously demonstrated by Redshaw et al.[5] Surprisingly, issues concerning the self-assembly process of oxozinc carboxylate clusters as well as the carboxylate ligand effect on this process have been rarely reported in the literature.[5,6] A variety of related oxozinc clusters supported by different organic ligands, like carboxylates,[5−7] carbamates,[8] amides,[9] or phosphonates,[10] have been prepared. However, lack of efficient and rational synthetic strategies leading to well-defined oxozinc complexes results in characterization of the products formed accidentally, and not as a consequence of a rational design. For instance, we reported on the synthesis of $[Zn_4(\mu_4\text{-}O)(O_2CPh)_6]$ through oxidation of the corresponding zinc carboxylate with dry oxygen,[6] whereas Redshaw et al. obtained an oxocarboxylate complex by reaction of $Zn(C_6F_5)_2$ with 3-dimethylaminobenzoic acid in the presence of trace amounts of water.[5] More recently, Schulz et al. reported the $[Zn_4(\mu_4\text{-}O)(O_2CCp^*)_6]$ formed by the direct carboxylation reaction of zincocene Cp^*_2Zn with CO_2.[11]

Herein we describe a novel effective and mild methodology for the synthesis of a series of oxozinc carboxylates involving well-defined alkylzinc precursors and H_2O. The subsequent study provides a direct picture of the influence of the substituent on the carboxylate ligand in generation of supramolecular architectures. Our structural analysis revealed that these discrete oxozinc clusters can form diverse types of noncovalent porous materials ranging from structures representing zeolitic topologies to soft porous materials with gated voids or open channels.

Alkylzinc carboxylates still represent an insufficiently explored family of organozinc compounds. Our group[6] and others[12] demonstrated that these complexes form various discrete polynuclear assemblies depending on the character of both the zinc-bonded substituents and the carboxylate ligands. In our search for effective synthetic methods of various metal oxide aggregates,[6,13] and encouraged by our recent results on the hydrolysis of zinc alkyls,[14] we designed and developed the following two-step reaction system for the atom-efficient preparation of $[Zn_4(\mu_4\text{-}O)(O_2CR)_6]$-type clusters, involving commercially available Et_2Zn, a carboxylic acid, and H_2O. In addition, the study was extended to examination of the

Received: April 30, 2012
Published: June 8, 2012

   dx.doi.org/10.1021/ic300864n | *Inorg. Chem.* 2012, 51, 7410−7414

noncovalent-interactions-driven self-assembly processes of the resulting series of oxozinc carboxylates.

RESULTS AND DISCUSSION

An Atom-Efficient Synthetic Method of Oxozinc Carboxylates. In a control experiment we added 2 mol equiv of Et_2Zn to 3 mol equiv of benzoic acid in THF, which resulted in the quantitative formation of a novel alkylzinc carboxylate $[\{EtZn(O_2CPh)\}\{Zn(O_2CPh)_2\}\cdot THF]$ (**1**) (Scheme 1).

Scheme 1

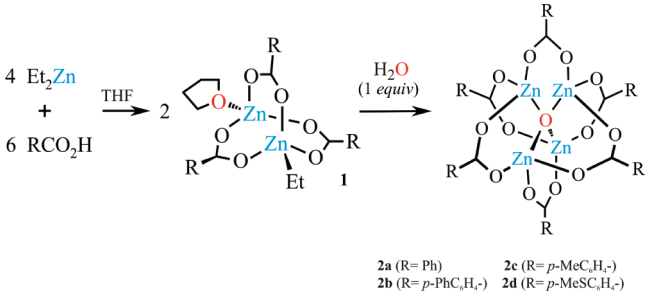

Compound **1** was isolated by crystallization from the postreaction mixture, and its structure was determined by spectral and X-ray single crystal studies. It crystallizes in a triclinic space group $P\bar{1}$ as a dinuclear cluster that can be formally treated as an adduct of ethylzinc benzoate $[EtZn(O_2CPh)]$ and zinc dibenzoate $[Zn(O_2CPh)_2]$ species. In the molecular structure of **1**, three carboxylate groups bridge two zinc atoms, nicely resembling a paddle-wheel motif with three puckered eight-membered $Zn_2O_4C_2$ rings (Figure 1). The

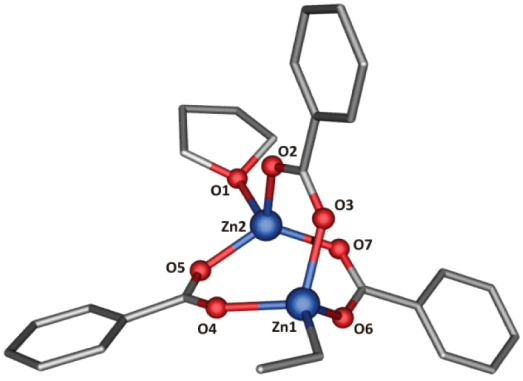

Figure 1. Molecular structure of **1**; hydrogen atoms have been omitted for clarity. Selected bond lengths (Å) and angles (deg): Zn1–O3, 2.017(9); Zn1–O4, 2.024(3); Zn1–O6, 2.045(1); Zn2–O1, 2.026(7); Zn2–O2, 1.944(1); Zn2–O5, 1.916(3); O4–Zn1–O3, 106.2(4); O4–Zn1–O6, 101.3(8); O1–Zn2–O2, 96.1(1); O2–Zn2–O5, 115.5(1).

metal centers represent a distorted tetrahedral coordination environment where Zn–O bond lengths fall within a range of 1.916–2.045 Å. It should be noted that **1** represents a new example of an alkylzinc carboxylate family, exhibiting vast structural variety.[12]

In the next step we carried out the reaction between **1** and H_2O in a molar ratio of 2:1 and in THF solution at ambient temperature for 12 h. From the postreaction mixture colorless icosahedral-shaped crystals of $[Zn_4(\mu_4\text{-}O)(O_2CPh)_6]$ (**2a**) were isolated at 4 °C in an almost quantitative yield. Encouraged by this result we extended our atom-efficient approach to the synthesis of a number of oxozinc clusters supported by other benzoic acid derivatives. We selected 4-methylbenzoic acid, 4-(methylthio)benzoic acid, and 4-biphenylcarboxylic acid as starting reagents in order to test the effect of substituents in position 4 on the noncovalent-driven self-assembly processes of the resulting oxozinc carboxylates.

A similar two-step synthetic procedure involving 2 equiv of Et_2Zn in THF and 3 equiv of the selected carboxylic acid (for the selection criterion vide infra) and followed by the addition of 0.5 equiv of H_2O yielded a series of isostructural oxozinc clusters $[Zn_4(\mu_4\text{-}O)(O_2CR)_6]$ [where R = *p*-PhC_6H_4 (**2b**), *p*-MeC_6H_4 (**2c**), and *p*-$MeSC_6H_4$ (**2d**)]. Compounds **2b–d** were isolated in high yields as cubic crystals, and the identity of the oxozinc carboxylates has been confirmed by X-ray crystallography (for experimental and crystallographic details see Experimental Section and Supporting Information). The identity of **2a** was confirmed by X-ray crystallography and proved to be consistent with the previous reports.[6] The structural analysis of **2b–d** revealed the presence of isostructural monomeric oxo-centered tetranuclear units with corresponding six μ-1,2-carboxylate bridges. In all cases, the central oxozinc core remained essentially unchanged, with the $Zn–O_{oxo}$ bond lengths falling into the range of 1.923–1.954 Å. However, the crystal structure analysis of these compounds provides interesting observations concerning the effect of the substituents' nature on the molecular self-assembly process of octahedral oxozinc clusters. It is noticeable that the corresponding geometric parameters in **2a–d** are very similar to those observed in the reported single crystal structure of MOF-5 (Table 1S, Supporting Information).[15]

Investigations on the Supramolecular Structures of 2a–d. A detailed analysis of the crystal structure of **2a** revealed that the Zn_4O clusters self-assemble through complementary specific noncovalent interactions to produce an extended 3D network with open-gated voids. From a topological point of view, the supramolecular structure of **2a** resembles that observed in the natural zeolite analcite (ANA) ($NaAlSi_2O_6\cdot H_2O$) (Figure 2a). On the basis of PLATON calculations,

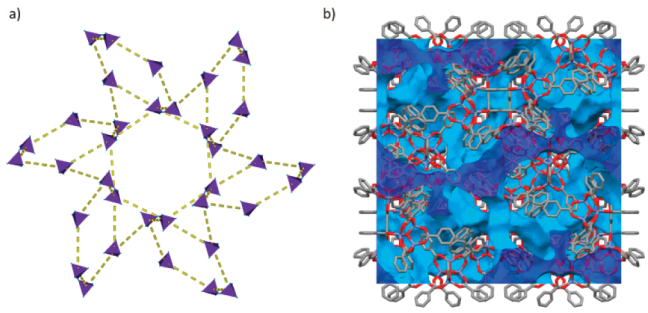

Figure 2. (a) Topological representation of **2a**. (b) Crystal packing structure for **2a** along the *a* axis and the solvent accessible areas; sky blue and navy blue represent the interior and exterior pore surface, respectively.

the accessible free voids in **2a** are estimated to be about 39.3% of the unit cell volume; however, these cages were inaccessible for gas molecules because of very small aperture sizes (vide infra), which is characteristic for analcite topology (Figure 2b).[16]

dx.doi.org/10.1021/ic300864n | Inorg. Chem. 2012, 51, 7410–7414

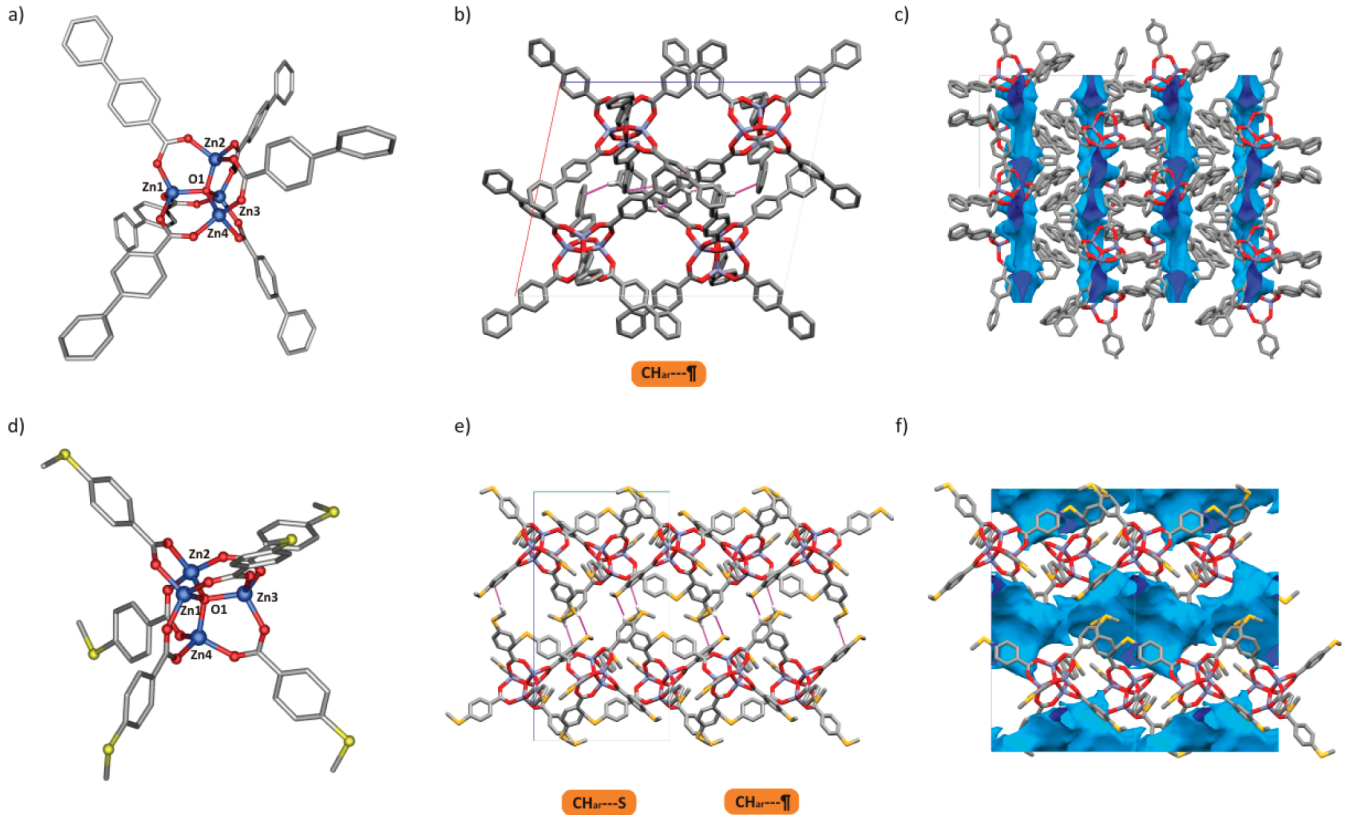

Figure 3. (a) Molecular structure of **2b**. (b) View of the supramolecular arrangement in a 2D grid of **2b** along the *b* axis. The purple lines represent C−H_{ar}···π cooperative interactions. Hydrogen atoms are omitted, excluding those involved in the nonconvalent interaction. (c) Crystal packing structure for **2b** along the *c* axis and the solvent accessible areas. (d) Molecular structure of **2d**. (e) View of the 2D zigzag-like network in the crystal structure of **2d** along the *a* axis showing the intermolecular CH_{ar}···S hydrogen bonds and CH_{ar}···π interactions (purple lines). (f) Crystal packing structure for **2d** along the *a* axis and the solvent accessible areas.

The observed 3D open framework structure with zeolite-like topology for **2a** encouraged us to employ the phenyl-substituted analogue of **2a**. We anticipated that the extension of the aromatic linkage may lead to significant changes in the molecular self-assembly of the oxozinc complex by increasing the spacing between vertices in a net and yielding an extended void space. Indeed, a closer examination of the structure of **2b** revealed that the Zn_4O clusters self-assemble via C−H_{ar}···π cooperative interactions to produce 2D grids with open channels directed along the *b* axis with diameter of ∼8 Å (Figure 3b). Unfortunately, these 2D grids are further organized by weak π···π stacking interactions into an extended 3D network featuring partially close packing of empty spaces in the crystal lattice (Figure 3c). PLATON calculation indicates an accessible volume of 23.4% upon solvent removal.

We also investigated the effect of methyl and methylthio substituents in the para-position of the carboxylate ligand on the supramolecular structure evolution and explored whether it could be used for further modification of the packing mode of the resulting noncovalent materials. A detailed analysis of the crystal structure of **2c** shows that hierarchical self-organization steps of these units driven by combination of noncovalent interactions lead to the formation of a 3D supramolecular network. The first level self-assembly process comprises the docking of four parent molecules of **2c**, which are held together by cooperative C−H_{ar}···O hydrogen bonds formed by aromatic hydrogen and carboxylate-oxygen atoms (with the distance of 2.718(6) Å), which results in the formation of the non-covalently bonded supertetrahedral cage, as illustrated in Figure 4a. These "secondary building modules" are further organized through a subsequent self-assembly process induced by C−H_{ar}···π interactions into an extended layered close-packed 3D structure with gated voids (Figure 4d). On the basis of PLATON calculations, the free voids in **2c** are estimated to constitute 31.3% of the unit cell volume; however, these voids are inaccessible due to the lack of connecting channels between them.

Upon the introduction of a donor atom to the substituent in the phenyl ring of **2d**, we expected further complications in the resulting supramolecular architecture as the sulfur atom can be involved in intra- and intermolecular noncovalent interactions. Indeed, adjacent molecular moieties of **2d** are interconnected by the intermolecular CH_{ar}···S hydrogen bonds between the sulfur and the hydrogen atoms of the aromatic ring (with the distance of 2.952 Å), leading to the H-bonded zigzag-like chain, as depicted in Figure 3e. Additionally, a network of intermolecular complementary CH_{ar}···π interactions resulted in the formation of 2D double layers lying on the (100) crystallographic plane. Thus, in the presence of the S−Me substituent, noncovalent interactions lead to the formation of the 2D framework with the existence of zigzag-like channels constituting 34% potential guest-accessible volume of the crystal volume based on the PLATON calculation (Figure 3f).

The degree of permanent porosity of **2a**−**d** was further verified by gas sorption measurements. In all cases attempts to evaluate an N_2 adsorption isotherm at 77 K revealed no significant uptake up to 1 bar, indicating the presence of gated voids in the host framework that blocks diffusion of N_2

dx.doi.org/10.1021/ic300864n | *Inorg. Chem.* 2012, 51, 7410−7414

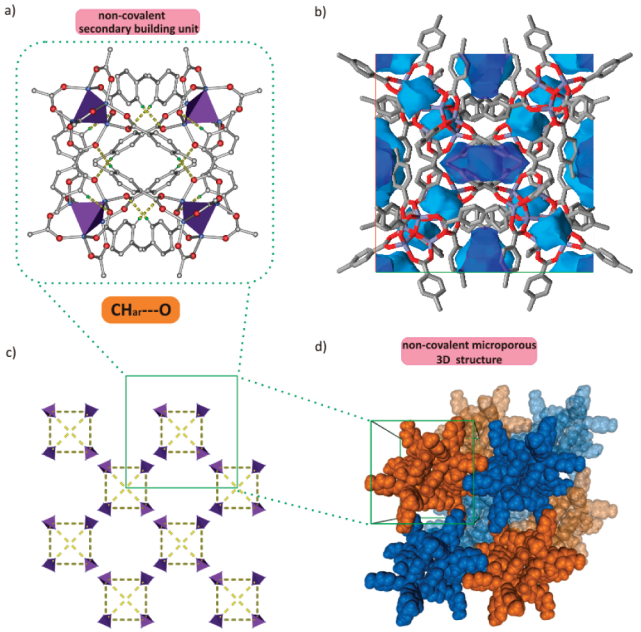

Figure 4. (a) View of the supertetrahedral cage of **2c** as a building module in the construction of extended 3D structure along the *a* axis; the purple lines represent C−H_{ar}···O cooperative interactions. Hydrogen atoms are omitted, excluding those involved in the nonconvalent interaction. (b) Crystal packing structure for **2c** along the *a* axis and the solvent accessible areas. (c) Topological representation of **2c**. (d) View of the extended 3D network in the crystal structure of **2c**.

molecules across the channel network;[17] however, the CO_2 adsorption studies for **2a** and **2b** at 273 K showed noticeable CO_2 uptakes of 10 cm^3 g^{-1} (1.8 and 2.1 wt %, respectively) at STP (Figure S5, Supporting Information). On the basis of the nonlocal density functional theory (NLDFT) method, the calculated surface areas for **2a** and **2b** were 90 and 95 m^2/g, respectively. Thus only a portion of available void spaces in the crystal lattice is available for gas molecules. The results indicate that the limiting pore diameter for these materials is higher than the kinetic diameter of CO_2, which may be due to structure collapse during activation process or to the need to apply a more efficient activation procedure.

■ CONCLUSIONS

In conclusion, we have developed a novel atom-efficient methodology for the synthesis of oxozinc carboxylates and a series of complexes $[Zn_4(\mu_4\text{-}O)(O_2CR)_6]$ [where R = *p*-MeC_6H_4 (**2b**), *p*-PhC_6H_4 (**2c**), *p*-MeC_6H_4 (**2d**)] was prepared and crystallographically characterized. We hope that this approach can be added as a convenient tool in the synthesis of well-defined oxozinc complexes. Our study revealed that these discrete clusters form diverse types of noncovalent assemblies, driven by the type of substituent in the aromatic ring, possessing void spaces or open channels. Further studies on the utilization of oxozinc carboxylates with purposefully functionalized carboxylate ligands as effective molecular building blocks for the construction of noncovalent porous materials are in progress.

■ EXPERIMENTAL SECTION

All manipulations were conducted under a nitrogen atmosphere by using standard Schlenk techniques. All reagents were purchased from commercial vendors. Solvents were dried and distilled prior to use. Redistilled water was degassed carefully by six freeze−pump−thaw cycles before use. NMR spectra were acquired on Varian Mercury 400 spectrometer.

Synthesis of 1. Et_2Zn (0.246 g, 2.00 mmol) was added to a suspension of benzoic acid (0.366 g, 3.00 mmol) in THF (10 mL) at −78 °C and then the reaction mixture was allowed to warm to 20 °C. Colorless plate crystals were obtained after crystallization from THF/toluene mixture at 20 °C; isolated yield ca. 89%. ^{1}H NMR ($CDCl_3$, 400.10 MHz, 298 K): δ = 0.19 (q, 2H; $ZnCH_2CH_3$), 1.08 (t, 3H; $ZnCH_2CH_3$), 1.89 (m, 4H; CH_2-THF), 3.86 (m, 4H; OCH_2-THF), 7.39 (m, 6H; Ar), 7.513 (m, 3H; Ar), 8.16 ppm (m, 6H; Ar). Anal. Calcd for $C_{27}H_{28}O_7Zn_2$: C, 54.52; H, 4.71. Found: C, 55.12; H, 4.97.

Synthesis of 2b. Et_2Zn (0.492 g, 4.00 mmol) was added to a suspension of 4-biphenylcarboxylic acid (1.19 g, 6.00 mmol) in THF (10 mL) at −78 °C. After 4 h, degassed H_2O (18 μL, 1.00 mmol) was added, and the solution was stirred for an additional 20 h. Colorless cubic crystals were isolated from a CH_2Cl_2 solution at −20 °C; isolated yield ca. 85%. ^{1}H NMR ($CDCl_3$, 400.10 MHz, 298 K): δ = 7.45−8.13 ppm (m, 54H; Ar). Anal. Calcd for $C_{78}H_{54}O_{13}Zn_4$: C, 64.14; H, 3.69. Found: C, 64.30; H, 3.87.

Synthesis of 2c. A similar procedure as for **2b** using *p*-toluic acid (0.810 g, 6.00 mmol) in THF and Et_2Zn (0.492 g, 4.00 mmol) in THF was used. All volatile compounds were removed under vacuum, and white powder was obtained. Colorless cubic crystals were isolated upon recrystallization from a THF solution at −20 °C; isolated yield ca. 89%. ^{1}H NMR ($CDCl_3$, 400.10 MHz, 298 K): δ = 2.38 (s, 3H; CH_3), 7.32 (m, 2H; Ar), 8.12 ppm (m, 2H; Ar). Anal. Calcd for $C_{48}H_{42}O_{13}Zn_4$: C, 52.98; H, 3.86. Found: C, 53.30; H, 3.97.

Synthesis of 2d. A similar procedure as for **2b** using 4-(methylthio)benzoic acid (1.01 g, 6.00 mmol) and Et_2Zn (0.492 g, 4.00 mmol) in THF was used. Yellow cubic crystals were isolated by crystallization from a THF solution at −20 °C; isolated yield ca. 87%. ^{1}H NMR ($CDCl_3$, 400.10 MHz, 298 K): δ = 2.40 (s, 3H; SCH_3), 7.28 (m, 2H; Ar), 7.94 ppm (m, 2H; Ar). Anal. Calcd for $C_{48}H_{42}O_{13}S_6Zn_4$: C, 45.02; H, 3.28; S, 15.02. Found: C, 45.35; H, 3.42; S, 14.87.

Crystallographic Data. The data were collected at 100(2) K on a Nonius Kappa CCD diffractometer[18] using graphite-monochromated Mo Kα radiation (λ = 0.710 73 Å). The unit cell parameters were determined from ten frames and then refined on all data. The data were processed with DENZO and SCALEPACK (HKL2000 package).[19] The structure was solved by direct methods using the SHELXS97[20] program and was refined by full-matrix least−squares on F2 using the program SHELXL97.[21] All non-hydrogen atoms were refined with anisotropic displacement parameters. The hydrogen atoms were introduced at geometrically idealized coordinates with a fixed isotropic displacement parameter equal to 1.5 (methyl groups) times the value of the equivalent isotropic displacement parameter of the parent carbon. Crystallographic data (excluding structure factors) for the structures reported in this paper have been deposited with the Cambridge Crystallographic Data Centre as supplementary publication no. CCDC-830646 (**1**), CCDC-878003 (**2b**), CCDC-830647 (**2c**), CCDC-830648 (**2d**). Copies of the data can be obtained free of charge on application to CCDC, 12 Union Road, Cambridge CB21EZ, UK [fax: (+44)1223−336−033; e-mail: deposit@ccdc.cam.ac.uk].

1: $C_{27}H_{28}O_7Zn_2$, M = 595.27, crystal dimensions 0.48 × 0.35 × 0.25 mm^3, triclinic, space group $P\bar{1}$ (No. 2), a = 9.9271(5) Å, b = 10.8259(4) Å c = 12.4851(7) Å, α = 97.652(3)°, β = 101.911(2)°, γ = 95.374(3)°, U = 1291.00(11) $Å^3$, Z = 2, F(000) = 612, D_c = 1.531 g m^3, T = 100(2)K, μ(Mo Kα) = 1.902 mm^{-1}, Nonius Kappa-CCD diffractometer, θ_{max} = 25.68°, 4820 unique reflections. Refinement converged at R1 = 0.0397, wR2 = 0.0698 for all data and 326 parameters [R1 = 0.0332, wR2 = 0.0673 for 4316 reflections with $I_o > 2\sigma(I_o)$]. The goodness-of-fit on F^2 was equal to 1.082. A weighting scheme $w = [\sigma^2(F_o^2 + (0.0418P)^2 + 3.1964P]^{-1}$ where $P = (F_o^2 + 2F_c^2)/3$ was used in the final stage of refinement. The residual electron density = +0.35/−0.42 e $Å^{-3}$

2b: $C_{78}H_{54}O_{13}Zn_4{\cdot}2CH_2Cl_2$, M = 1630.63, crystal dimensions 0.44 × 0.32 × 0.26 mm^3, monoclinic, space group $P2_1/c$ (No. 14), a = 20.7641(8) Å, b = 14.8559(4) Å c = 25.5201(9) Å, β = 102.0510(10)°,

dx.doi.org/10.1021/ic300864n | Inorg. Chem. 2012, 51, 7410−7414

U = 7698.7(5) Å^3, Z = 4, F(000) = 3320, D_c = 1.407 g m^3, T = 100(2)K, μ(Mo Kα) = 1.430 mm^{-1}, Nonius Kappa-CCD diffractometer, θ_{max} = 22.46°, 9871 unique reflections. Refinement converged at R1 = 0.0940, wR2 = 0.1644 for all data and 910 parameters [R1 = 0.0552, wR2 = 0.1310 for 7190 reflections with $I_o > 2\sigma(I_o)$]. The goodness-of-fit on F^2 was equal to 1.061. A weighting scheme $w = [\sigma^2(F_o^2 + (0.0418P)^2 + 3.1964P]^{-1}$ where $P = (F_o^2 + 2F_c^2)/3$ was used in the final stage of refinement. The residual electron density = +0.73/−0.87 e Å^{-3}.

2c: $C_{48}H_{42}O_{13}Zn_4$, M = 1088.38, crystal dimensions 0.44 × 0.36 × 0.30 mm^3, cubic, space group $I23/c$ (No. 197), a = 23.034(5) Å, U = 12221(5) Å^3, Z = 8, F(000) = 4432, D_c = 1.183 g m^3, T = 100(2)K, μ(Mo Kα) = 1.600 mm^{-1}, Nonius Kappa-CCD diffractometer, θ_{max} = 27.93°, 4751 unique reflections. Refinement converged at R1 = 0.0677, wR2 = 0.1189 for all data and 199 parameters (R1 = 0.0474, wR2 = 0.1116 for 3728 reflections with $I_o > 2\sigma(I_o)$). The goodness-of-fit on F^2 was equal to 1.102. A weighting scheme $w = [\sigma^2(F_o^2 + (0.0418P)^2 + 3.1964P]^{-1}$ where $P = (F_o^2 + 2F_c^2)/3$ was used in the final stage of refinement. The residual electron density = +0.46/−0.39 e Å^{-3}.

2d: $C_{48}H_{42}O_{13}S_6Zn_4$, M = 1280.31, crystal dimensions 0.44 × 0.38 × 0.34 mm^3, monoclinic, space group $P21/c$ (No. 14), a = 14.1301(8) Å, b = 16.5959(5) Å, c = 30.8969(16) Å, β = 101.998(2)°, U = 7087.1(6) Å^3, Z = 4, F(000) = 2600, D_c = 1.200 g m^3, T = 100(2)K, μ(Mo Kα) = 1.560 mm^{-1}, Nonius Kappa-CCD diffractometer, θ_{max} = 23.25°, 9890 unique reflections. Refinement converged at R1 = 0.0952, wR2 = 0.1409 for all data and 646 parameters (R1 = 0.0577, wR2 = 0.1298 for 6095 reflections with $I_o > 2\sigma(I_o)$). The goodness-of-fit on F^2 was equal to 0.931. A weighting scheme $w = [\sigma^2(F_o^2 + (0.0418P)^2 + 3.1964P]^{-1}$ where $P = (F_o^2 + 2F_c^2)/3$ was used in the final stage of refinement. The residual electron density = +0.77/−0.57 e Å^{-3}.

■ ASSOCIATED CONTENT

Ⓢ Supporting Information

X-ray crystallographic files in CIF format, molecular figures, and bond length/bond angle tables for compounds **1a** and **2b**−**d**. This material is available free of charge via the Internet at http://pubs.acs.org.

■ AUTHOR INFORMATION

Corresponding Author

*E-mail: lewin@ch.pw.edu.pl.

Notes

The authors declare no competing financial interest.

■ ACKNOWLEDGMENTS

The authors would like to acknowledge the Ministry of Science and Higher Education: projects N N204 142237 (W.B.) and N N204 164336 and the European Union in the framework through the Warsaw University of Technology Development Programme of ESF (D.P.) for financial support.

■ REFERENCES

(1) (a) Li, H.; Eddaoudi, M.; O'Keeffe, M.; Yaghi, O. M. *Nature* **1999**, *402*, 276−279. (b) Eddaoudi, M.; Moler, D. B.; Li, H.; Chen, B.; Reineke, T. M.; O'Keeffe, M.; Yaghi, O. M. *Acc. Chem. Res.* **2001**, *34*, 319−330.

(2) Hausdorf, S.; Baitalow, F.; Boehle, T.; Rafaja, D.; Mertens, F. O. R. L. *J. Am. Chem. Soc.* **2010**, *132*, 10978−10981.

(3) For selected examples see: (a) Rosi, N. L.; Eckert, J.; Eddaoudi, M.; Vodak, D. T.; Kim, J.; O'Keeffe, M.; Yaghi, O. M. *Science* **2003**, *300*, 1127−1129. (b) Rowsell, J. L. C.; Yaghi, O. M. *Angew. Chem., Int. Ed.* **2005**, *44*, 4670−4679. (c) Férey, G. *Chem. Soc. Rev.* **2008**, *37*, 191−214. (d) Suh, M. P.; Park, H. J.; Prasad, T. K.; Lim, D.-W. *Chem. Rev.* **2012**, *112*, 782−835.

(4) (a) Rowsell, J. L. C.; Spencer, E. C.; Eckert, J.; Howard, J. A. K.; Yaghi, O. M. *Science* **2005**, *309*, 1350−1354. (b) Rowsell, J. L. C.; Eckert, J.; Yaghi, O. M. *J. Am. Chem. Soc.* **2005**, *127*, 14904−14910. (c) Spencer, E. C.; Howard, J. A. K.; McIntyre, G. J.; Rowsell, J. L. C.; Yaghi, O. M. *Chem. Commun.* **2006**, 278−280.

(5) Redshaw, C.; Jana, S.; Shang, C.; Elsegood, M. R. J.; Lu, X.; Guo, Z. X. *Organometallics* **2010**, *29*, 6129−6132.

(6) Lewiński, J.; Bury, W.; Dutkiewicz, M.; Maurin, M.; Justyniak, I.; Lipkowski, J. *Angew. Chem., Int. Ed.* **2008**, *47*, 573−576.

(7) (a) Hiltunen, L.; Leskela, M.; Makela, M.; Niinisto, L. *Acta Chem. Scand. A* **1987**, *41*, 548−550. (b) Clegg, W.; Harbron, D. R.; Homan, C. D.; Hunt, P. A.; Little, I. R.; Straughan, B. P. *Inorg. Chim. Acta* **1991**, *186*, 51−60. (c) Yin, M. C.; Wang, C. W.; Sun, J. T. *Chin. J. Lumin.* **2003**, *24*, 485−488. (d) Otvös, S. B.; Berkesi, O.; Körtvélyesi, T.; Pálinkó, I. *Inorg. Chem.* **2010**, *49*, 4620−4625.

(8) McCowan, C. S.; Groy, T. L.; Caudle, M. T. *Inorg. Chem.* **2002**, *41*, 1120−1127.

(9) Davies, R. P.; Linton, D. J.; Schooler, P.; Snaith, R.; Wheatley, A. E. H. *Chem.—Eur. J.* **2001**, *7*, 3696−3704.

(10) Yang, Y.; Pinkas, J.; Noltemeyer, M.; Schmidt, H.−G.; Roesky, H. W. *Angew. Chem., Int. Ed.* **1999**, *38*, 664−666.

(11) Schulz, S.; Schmidt, S.; Bläser, D.; Wölper, C. *Eur. J. Inorg. Chem.* **2011**, *27*, 4157−4160.

(12) (a) Dickie, D. A.; Jennings, M. C.; Jenkins, H. A.; Clyburne, J. A. C. *Inorg. Chem.* **2005**, *44*, 828−830. (b) Redshaw, C.; Elsegood, M. R. *Angew. Chem., Int. Ed.* **2007**, *46*, 7453−7457. (c) Orchard, K. L.; White, A. J. P.; Shaffer, M. S. P.; Williams, C. K. *Organometallics* **2009**, *28*, 5828−5832. (d) Redshaw, C.; Elsegood, M. R. J.; Frese, J. W. A.; Ashby, S.; Chao, Y.; Mueller, A. *Chem. Commun.* **2012**, DOI: 10.1039/c2cc32060f. (e) Orchard, K. L.; Harris, J. E.; White, A. J. P.; Shaffer, M. S. P.; Williams, C. K. *Organometallics* **2011**, *30*, 2223−2229.

(13) Al oxo clusters: (a) Lewiński, J.; Bury, W.; Justyniak, I.; Lipkowski, J. *Angew. Chem., Int. Ed.* **2006**, *45*, 2872−2875. (b) Bury, W.; Chwojnowska, E.; Justyniak, I.; Lewiński, J.; Affek, A.; Zygadło-Monikowska, E.; Bąk, J.; Florjańczyk, Z. *Inorg. Chem.* **2012**, *51*, 737−745. Zn oxo clusters: (c) Lewiński, J.; Suwała, K.; Kaczorowski, T.; Gałęzowski, M.; Gryko, D. T.; Justyniak, I.; Lipkowski, J. *Chem. Commun.* **2009**, 215−217. (d) Sokołowski, K.; Justyniak, I.; Śliwiński, W.; Sołtys, K.; Tulewicz, A.; Kornowicz, A.; Lipkowski, J.; Moszyński, R.; Lewiński, J. *Chem.—Eur. J.* **2012**, *18*, 5637−5645. (e) Zelga, K.; Leszczyński, M.; Justyniak, I.; Kornowicz, A.; Cabaj, M.; Wheatley, A. E. H.; Lewiński, J. *Dalton Trans.* **2012**, *41*, 5934−5938.

(14) Bury, W.; Krajewska, E.; Dutkiewicz, M.; Sokołowski, K.; Justyniak, I.; Kaszkur, Z.; Kurzydłowski, K. J.; Płociński, T.; Lewiński, J. *Chem. Commun.* **2011**, *19*, 5467−5469.

(15) Eddaoudi, M.; Kim, J.; Rosi, N.; Vodak, D.; Wachter, J.; O'Keeffe, M.; Yaghi, O. M. *Science* **2002**, *295*, 469−472.

(16) For the Database of Zeolite Structures, please see: www.iza-structure.org/databases/.

(17) We note that the structures have not collapsed during the adsorption, as indicated by PXRD measurements of the bulk materials.

(18) *KappaCCD Software*; Nonius B.V.: Delft, The Netherlands, 1998.

(19) Otwinowski, Z.; Minor, W. *Methods Enzymol.* **1997**, *276*, 307.

(20) Sheldrick, G. M. *Acta Crystallogr., Sect. A* **1990**, 467−473.

(21) Sheldrick, G. M. *SHELXL97*; University Göttingen, Germany, 1997.